Computer Aided Modeling for a Miniature Silicon-on-Insulator MEMS Piezoresistive Pressure Sensor

K. J. SUJA* and Rama KOMARAGIRI

Department of ECE, National Institute of Technology, Calicut, India

*Corresponding author: K. J. SUJA E-mail: suja@nitc.ac.in

Abstract: The silicon-on-insulator diaphragm structure is a combined structure of the silicon dioxide and silicon layer. This work presents a new method to estimate the deflection response of silicon with that of a silicon-on-insulator (SOI) diaphragm structure, based on the burst pressure design approach. It also evaluates the output voltage of the diaphragm under two different conditions, flipped and un-flipped. The new modified analytical model developed and presented in this paper for describing the load deflection of SOI diaphragm is able to predict the deflection accurately when compared with the results obtained by finite element analysis CoventorWare®.

Keywords: Micro electro mechanical system (MEMS), finite element analysis (FEA), stacked diaphragm, sensitivity

Citation: K. J. SUJA and Rama KOMARAGIRI, "Computer Aided Modeling for a Miniature Silicon-on-Insulator MEMS Piezoresistive Pressure Sensor," *Photonic Sensors*, 2015, 5(3): 202–210.

1. Introduction

A wide range of improvement in the silicon integrated circuits and micromachining technology has enabled the development of various sensing instruments. The micro electro mechanical system (MEMS) pressure sensors are the most widely used MEMS devices and they constitute a major share in the MEMS market [1]. The design of MEMS piezoresistive pressure sensor extensively adopts finite element analysis (FEA) to realize stress distribution for reliability, sensitivity, and non-linearity [2]. Most of the piezoresistive pressure sensors use silicon as a diaphragm and piezoresistive property of silicon or polycrystalline silicon to sense the pressure [3–5]. A silicon MEMS pressure sensor which changes the capacitance as a sensing mechanism has been widely reported [6–8]. The use of a square diaphragm for pressure sensing is preferred because it has better sensitivity than a circular diaphragm [9]. Piezoresistive gauges aligned in the (111) direction on a {110} plane square diaphragm with central boss was found to give better sensitivity [10]. By knowing the pressure range, which is a design specification, the sensitivity of a piezoresistive sensor can be optimized by optimizing the diaphragm thickness and other dimensions. When a thin diaphragm is subjected to high pressure, it may result in large deflections and will induce non-linearity [11]. Based on the silicon piezoresistive effect and properties of elasticity, one can manufacture pressure sensors by microelectronic integrated manufacturing techniques. Piezoresistivity is a material property in which the bulk resistivity is influenced by the mechanical stress applied to the material. The resistivity of a material

Received version: 8 January 2015 / Revised version: 18 March 2015
© The Authors(s) 2015.This article is published with open access at Springerlink.com
DOI: 10.1007/s13320-015-0239-y
Article type: Regualr

depends on the internal atom positions and their motions. Strain changes the arrangement of atoms and hence the bulk resistivity. Moreover, the MEMS technology allows more electronics to be fabricated on the same chip [12] along with a transducer for compact and more built-in intelligence features. Figure 1 shows the placement of piezoresistors on a silicon pressure sensor diaphragm that can be manufactured by using the surface micromachining technology. By changing the position of piezoresistors, the output voltage of the bridge can be changed so that there is an improvement in the sensitivity. It has been reported that the longitudinal and transversal gauges can be divided into two or more parts in order to improve the sensor sensitivity [13]. The placement of piezoresistors (R_1–R_4) is such that each resistor is placed at the maximum stress locations on the diaphragm as shown in Fig. 1. These four piezoresistors are connected in a wheat stone bridge configuration. When a pressure is applied, due to the induced stress, the resistance of resistor changes and the bridge is out of balance which results in an output voltage. If V_{in} is the input voltage to the bridge, the output voltage V_{out} which is proportional to the applied pressure is given by (1). When a pressure is applied, the diffused piezoresistors on the top of the silicon layer sense the induced stress.

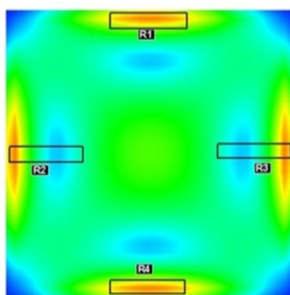

Fig. 1 Placement of resistors on the square diaphragm.

$$V_{out} = \left(\frac{R_3}{R_1 + R_3} - \frac{R_4}{R_2 + R_4} \right) V_{in} . \qquad (1)$$

In order to achieve a better sensitivity, optimizing the load-deflection characteristics of the diaphragm is the most important requirement. The diaphragm thickness should be as low as possible for a higher sensitivity. However, the diaphragm thickness should be designed in such a way that the continuous application of the maximum allowable pressure should not damage the diaphragm. In this condition, the resultant induced stress should be less than the maximum induced stress. By considering the burst pressure, one can reduce the non-linearity in the diaphragm if the deflection of the diaphragm is limited to one fifth of the diaphragm thickness. An applied pressure (P) in Pascal sensitivity can be expressed as

$$s = \frac{V_{out}}{V_{in} P} \text{mV} / \text{V} \cdot \text{Pa} . \qquad (2)$$

For a given burst pressure, an effective design should result in higher sensitivity by maximizing a pressure-deflection response considering both side length and thickness of a diaphragm. The systematic design methodology for the deflection of silicon on insulator (SOI) pressure sensors is rarely reported in the literature even though the fabrication of pressure sensors realized on silicon on insulator wafers have been widely reported. An effective design should attempt to achieve higher sensitivity by maximizing pressure-deflection response considering both side length and thickness for the given burst pressure. Higher sensitivity can be achieved by implementing the double diaphragm based pressure sensors [14]. The existing theory for the deflection response of the stacked diaphragm structure evaluates the deflection only at the maximum point [15]. The new method presents a different approach to design a high sensitive diaphragm type pressure sensor that uses an insulator on the diaphragms. The thickness of insulator plays an important role in the deflection. By varying the thickness of the insulator, the deflection can be varied, and as a result the sensitivity changes. If silicon dioxide is used as the insulator, the oxide is called as the buried oxide (BOX).

2. Design criteria in MEMS pressure sensor

The load deflection method that describes the relation between the displacement and applied pressure for a flat square diaphragm is given by (3) [16].

$$\frac{Pl^4}{Eh^4}=\frac{4.2}{\left(1-v^2\right)}\left(\frac{y}{h}\right)+\frac{1.58}{\left(1-v^2\right)}\left(\frac{y}{h}\right)^3 \tag{3}$$

where E is Young's modulus, v is Poisson's ratio of the diaphragm material, l is the side length of the diaphragm in μm, and h is the diaphragm thickness in μm. According to the load-deflection method, the deflection range is divided into two regions, namely, a small deflection region (deflection less than 25% of the diaphragm thickness) described by the linear term in (3) and a large deflection region (deflection greater than 25% of the diaphragm thickness) described by the non-linear, cubic term in (3). Due to symmetry, the square diaphragm has the highest induced stress for a given applied pressure. Thus the square diaphragm is preferred for the design of a pressure sensor. For a square plate clamped at the edges, the maximum stress ($\sigma_{\max}$) [17] at the center of the each edge is given by (4).

$$\sigma_{\max}=\frac{0.308Pl^4}{h^2}. \tag{4}$$

The maximum deflection in the diaphragm is given by (5)

$$w_{\max}=\frac{-0.0138Pl^4}{Eh^3}. \tag{5}$$

The deflection and stress on the diaphragm play an important role in analyzing the performance of the diaphragm.

3. Performance analysis of MEMS pressure sensor

The pressure sensors work on the principle of mechanical deformation and stress, induced by the application of the applied pressure. The deformation induces stresses which are then converted into the electrical signal output through some means of transduction. The pressure sensors have evacuated cavity which is generated by some means of micromachining on one side of the diaphragm. The deflection analysis of diaphragm having a side length of 500 μm and thickness of 15 μm for a burst pressure of 10 MPa is shown in Fig. 2. The maximum pressure applied is 0.9 MPa which is less than the one tenth of the burst pressure used for calculating the minimum diaphragm thickness. The maximum stress induced is one tenth of the fracture stress as expected. FEA tool CoventorWare® is used to build the pressure sensor structure and the results predict the deflection. The deflection in the diaphragm as a function of applied pressure is shown in Fig. 2. A comparison between analytical and FEA simulations is done and is shown in Fig. 2. It can be noted that the analytical results and FEA simulations match pretty well.

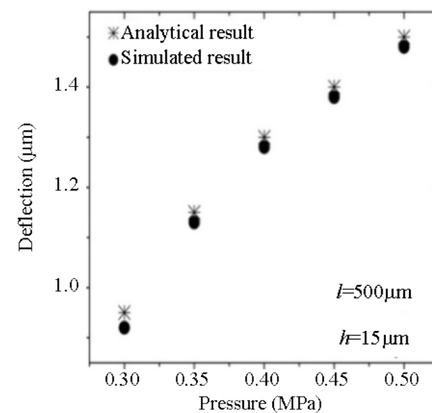

Fig. 2 Deflection analysis of silicon pressure sensor as a function of pressure.

For a square diaphragm, the maximum displacement is at the center of the diaphragm, and the maximum stress location is at the center of the edge.

4. Merit of SOI over silicon diaphragm

The schematic cross section of an SOI technology based MEMS pressure sensor implemented by the surface micromachining process is shown in Fig. 3. The conventional silicon diaphragm is realized by bulk micromachining, and the vertical and horizontal edges of the diaphragm

are essentially an integral part of the substrate. In contrast to this, the diaphragm in the SOI pressure sensor is realized by surface micromachining and the vertical and horizontal edges of the diaphragm are not an integral part of the substrate.

The total thickness h of the diaphragm is the sum of insulator thickness h_1 and silicon layer thickness h_2 as shown in Fig. 3. The piezoresistors are diffused on the top silicon layer which senses the induced stress. In the present work, the diaphragm material is made of n-type doped silicon. The implanted piezoresistors in the diaphragm are p-type doped silicon. The n-diaphragm and p-piezoresistor form a pn junction. The pn junction isolates the electrical path between the diaphragm and resistor. The advantages of the SOI diaphragm are that the pn junction leakage current can be reduced to zero. So that greater deflection and sensitivity is obtained from SOI diaphragm structures. Fig. 4 shows the deflection of SOI and silicon diaphragms for the same dimensions (500 μm, 600 μm, and 700 μm) and the same applied pressure.

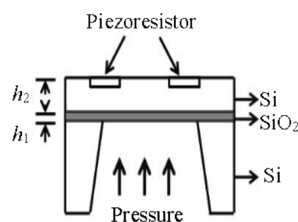

Fig. 3 Schematic of SOI pressure sensor diaphragm.

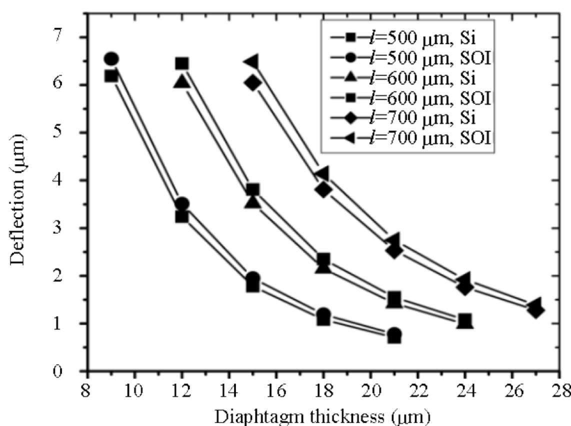

Fig. 4 Comparison of deflection in silicon and SOI diaphragm as a function of diaphragm thickness.

From Fig. 4, it can be noted that the deflection in an SOI diaphragm is more when compared with the silicon diaphragm with the same dimensions. In order to analyze the deflection, three structures having different dimensions have been considered. It is also found that the output voltage of the pressure sensor using an SOI diaphragm is greater than that of the silicon diaphragm since the deflection obtained is greater in the SOI diaphragm. Hence, the sensitivity of the SOI diaphragm increases when compared with that of a silicon diaphragm.

5. Issues with the application of load deflection formulae to the SOI structure

There are issues with applying the above said theory to pressure sensors realized on the SOI structure depicted in Fig. 3. The direct application of the existing analytical model to the SOI structure may not be accurate since the buried SiO_2 layer between the substrate and the diaphragm is not considered in this model. In such a situation, FEA is an efficient design tool since it can estimate the deflection and total stress developed in the diaphragm irrespective of the structure and dimensions of the various layers.

Fig. 5 shows the deflection of an SOI diaphragm with a side length 500 μm and a total diaphragm thickness of 15 μm. The buried oxide thickness is 10% of the total diaphragm thickness. The deflection shows a linear variation over the applied pressure ranges, and this indicates that the diaphragm is in a small deflection regime. For a side length of 500 μm and total diaphragm thickness of 15 μm, the deflection increases as the percentage of SiO_2 layer increases. It should be noted that the total thickness of the SOI diaphragm "h" remains constant, and a change in h_1 results in a change in h_2. The FEA simulation results having various SiO_2 thicknesses are shown in Fig. 6. By increasing the SiO_2 thickness, the deflection increases, and also it is evident that the SiO_2 thickness has a significant role in deciding the deflection of the diaphragm.

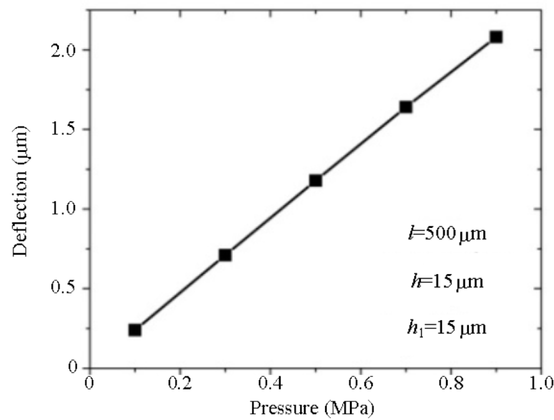

Fig. 5 Deflection in an SOI diaphragm.

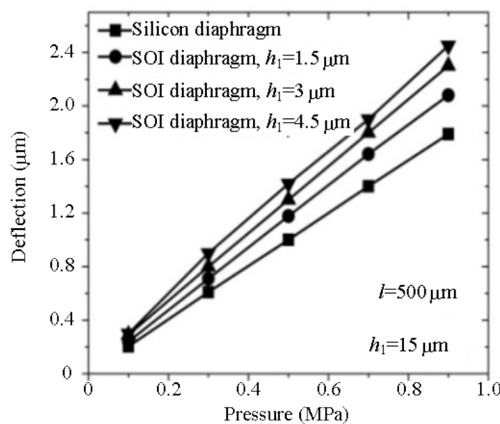

Fig. 6 Comparison of deflection in SOI as a function of applied pressure.

6. Analysis of flipped structure

In order to analyze the deflection, a flipped diaphragm structure is considered which is shown in Fig. 7. A flipped diaphragm is formed by stacking the silicon layer first and stacking the oxide layer on the top of the silicon layer.

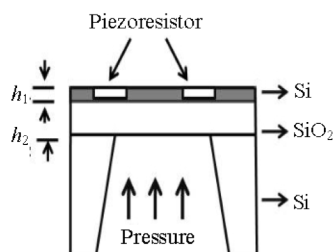

Fig. 7 Schematic cross section of flipped SOI diaphragm.

The performances of a flipped and un-flipped (ordinary) diaphragm structure such as deflection in a diaphragm, and the sensor output voltage are studied. Comparing Figs. 3 and 7, the main difference between flipped and un-flipped diaphragms is the relative position of Si and SiO_2 layers. There is no difference in the design parameters or the structural dimensions between the flipped and un-flipped diaphragms. The design parameters and material parameters used in this study are listed in Table 1. Fig. 8 shows a comparison of the deflection between flipped and un-flipped diaphragms with a side length of 500 μm, a total diaphragm thickness of 15 μm, and an applied pressure of 0.9 MPa.

Table 1 Design Parameters of un-flipped and flipped diaphragm.

Parameter	Value
Diaphragm side length (l)	500 μm
Diaphragm thickness (h)	15 μm
Resistors of (R_1–R_4)	2.5 kΩ
Resistivity (ρ)	2 Ω·cm

In the flipped structure, as the thickness of the insulation layer increases, the deflection increases as the pressure increases as shown in Fig. 8, and then it saturates at higher values of an applied pressure. When compared with an un-flipped diaphragm, the deflection in the flipped diaphragm remains exactly matched with that of the un-flipped diaphragm.

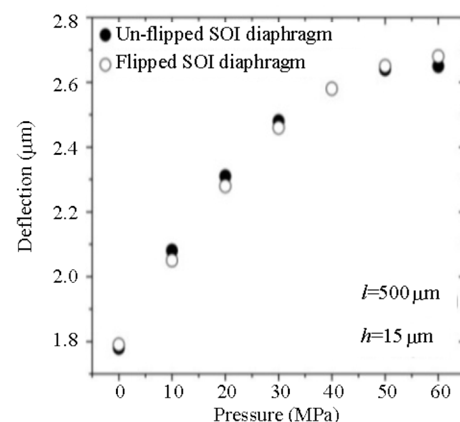

Fig. 8 Comparison of deflection in flipped and un-flipped diaphragms.

As shown in Fig. 9, the sensor output voltage is significantly smaller in the case of flipped structure.

There is a significant difference in the output voltage of the flipped diaphragm structure when compared with that of the un-flipped diaphragm structure. The difference in the behavior between the flipped and un-flipped diaphragm structures can be explained in the following way. In the flipped structure, the stress is first transferred into an SiO_2 layer which is amorphous and then into the silicon layer. As the stress relaxes in the SiO_2 layer, the piezoresistors encounter less stress, thus reducing the output voltage of the sensor. Since the diaphragm dimensions and materials used for the flipped structure are the same as that for the un-flipped structure, the structural rigidity of both the diaphragms is the same. Hence the deflection of the flipped structure is the same as that of the un-flipped diaphragm structure for different oxide layer thicknesses. As shown earlier in Fig. 9, as the oxide layer thickness increases initially the deflection increases and gets saturated at high insulation layer thicknesses. In the case of flipping structure, the stress is more relaxed when compared with the stress in the un-flipped structure. This is due to the fact that in the flipped structure the stress is generated by an amorphous material while in the case of un-flipped structure the stress is resulted from a crystalline layer. Thus, it can be concluded that the difference in the stress generation is responsible for the huge change in the sensor output voltage.

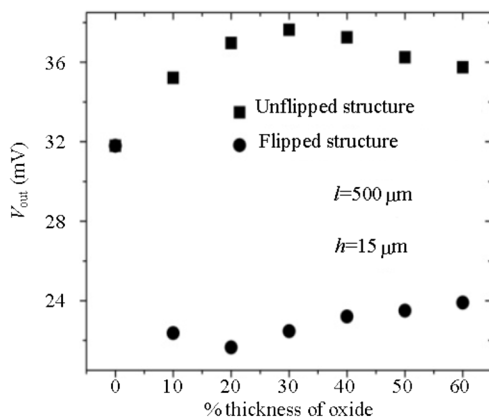

Fig. 9. Comparison of output voltage of flipped and un-flipped diaphragms.

7. Analytical model for the deflection of SOI diaphragm

The results of the burst pressure based design approach can be said to be valid only if the results predicted by FEA simulation matches with the results predicted by the analytical model. The authors have used both approaches to validate the simulation results presented in this paper. Fig. 10 shows the condition of a bar or diaphragm under the action of an axial force. The load or pressure is applied uniformly along the whole length of the diaphragm. The magnitude of s is such as to prevent the ends of the bar moving along the axis.

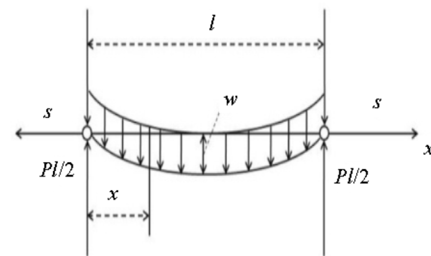

Fig. 10 Uniformly loaded plate with simply supported edges.

For a uniformly loaded diaphragm with simply supported edges, the bending moment at any cross section of the strip is given by (6) [17].

$$M=\frac{Pl}{2}x-\frac{Px^2}{2}-sw \tag{6}$$

where s is the axial force, P is the applied load, l is the length of the plate, and w is the displacement. For a thin plate, the flexural rigidity D of the diaphragm can be expressed as

$$D\frac{d^2w}{dx^2}=-M. \tag{7}$$

Substituting (6) into (7), we have

$$\frac{d^2w}{dx^2}-\frac{sw}{D}=-\frac{Plx}{2D}+\frac{Px^2}{2D} \tag{8}$$

and introduce the notation

$$\frac{sl^2}{4D}=u \tag{9}$$

$$w = C_1 \sinh \frac{2ux}{l} + C_2 \cosh \frac{2ux}{l} + \frac{Pl^3 x}{8u^2 D} - \frac{Pl^2 x^2}{8u^2 D} - \frac{Pl^4}{16u^4 D}. \quad (10)$$

The constants of integration C_1 and C_2 can be determined from the conditions at the ends of the SOI diaphragm. The deflection of the diaphragm at the ends are zero i.e., w=0 for x=0 and x=l. The deflection is the maximum at the center of the diaphragm and can be obtained by substituting x=l/2 in (11).

$$w = \frac{Pl^4}{16u^4 D}\left[\frac{\cosh u\left(1-\frac{2x}{l}\right)}{\cosh u} - 1\right] + \frac{Pl^2 x(l-x)}{8u^2 D}. \quad (11)$$

The bending rigidity of the composite diaphragm is given by (12) [18].

$$D = \frac{E_1 h_1^3}{12\left(1-v_1^2\right)} + \frac{E_2 h_2^3}{12\left(1-v_2^2\right)} \quad (12)$$

with h=h_1+h_2. The deflection is the maximum at the center of the diaphragm and can be obtained by substituting $x = l/2$ and is given by

$$w_{\max} = \frac{5Pl^4}{384D} f_0(u) \quad (13)$$

where $f_0(u)$ needs to be determined graphically [17]. The final expression for the maximum deflection by substituting D can be expressed as that in (14).

$$w_{\max} = 0.8Pl4\left[\frac{E_1 h_1^3}{12\left(1-v_1^2\right)} + \frac{E_2 h_2^3}{12\left(1-v_2^2\right)}\right]. \quad (14)$$

The load deflection relation has been used to estimate the deflection analytically and compared with the FEA simulation results. The same Young's module (E), Poisson ratio (v), and density (ρ_v) of the SiO_2 and the silicon layers of the diaphragm assumed in the FEA simulation studies have also been used in the analytical calculations. The analytical deflection values obtained at different pressures using the modified analytical model reported in this paper have been analyzed along with the deflection obtained through FEA simulation studies. Fig. 11 shows the deflection of diaphragm having a dimension of side length (l) of 500 µm and total diaphragm thickness (h) of 15 µm, which is found to be more for the diaphragm with BOX. The analytical deflection values obtained at different pressures using the modified analytical model have been analyzed with different thicknesses of 4.5 µm and 3 µm. From Fig. 12, it is clear that the deflection increases with the BOX thickness.

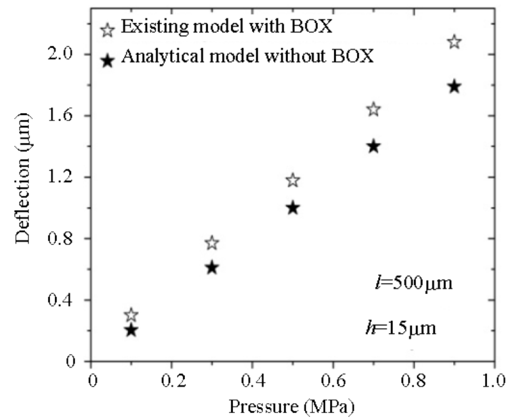

Fig. 11 Comparison of deflection between FEA model and existing model.

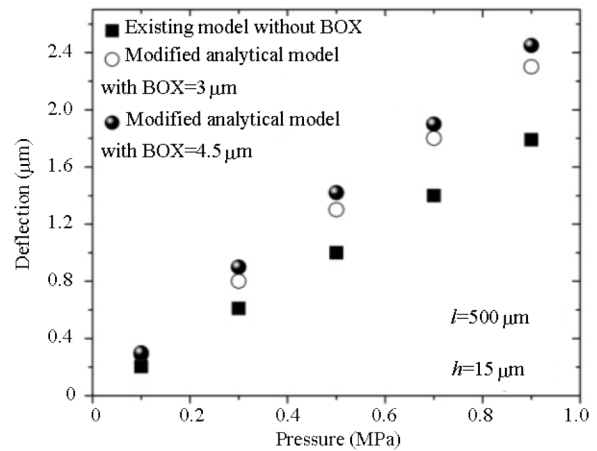

Fig. 12 Comparison of deflection between existing model and FEA with different BOX thicknesses.

Figure 13 shows the deflection for a side length of 500 μm and a thickness of 15 μm with a particular BOX thickness. In addition to the results reported in the literature, this work evaluates the deflection at every point on the diaphragm as shown in Fig. 14. Compared with the results reported in the literature, which is the only reported one for a stacked diaphragm, this is a new approach for deflection analysis. Comparison of the present work with the existing work is summarized in Table 2.

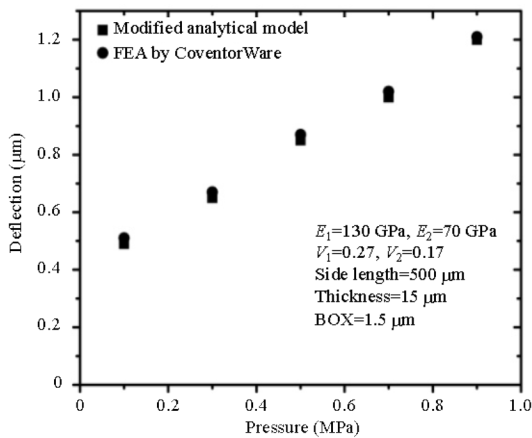

Fig. 13 Comparison of modified analytical model and FEA with CoventorWare.

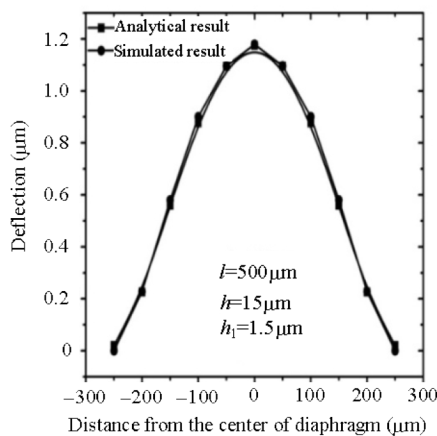

Fig. 14 Longitudinal deflection profiles.

Table 2 Comparison of the FEA simulated results with reported results [15].

	Expression for deflection	Analysis of sensor diaphragm
Narayanswami *et al.* [15]	Evaluates the maximum deflection of the diaphragm	Evaluates the deflection of un-flipped diaphragm
New analytical expression	In addition to the maximum deflection, evaluates the deflection along the whole length of the diaphragm	Evaluates the deflection of both flipped and un-flipped diaphragms

Acknowledgment

The author gratefully acknowledges the support from the authorities of the National Program on Micro and Smart Systems (NPMass) in terms of MEMS Software design tools.

Open Access This article is distributed under the terms of the Creative Commons Attribution License which permits any use, distribution, and reproduction in any medium, provided the original author(s) and source are credited.

References

[1] Y. Zhang, C. Yang, Z. Zhang, H. Lin, L. Liu, and T. Ren, "A novel pressure micro sensor with 30-μm–thick diaphragm and meander-shaped piezoresistors partially distributed on high-stress bulk silicon region," *IEEE Sensors Journal*, 2007, 7(12): 1742–1748.

[2] L. Lin and W. Yun, "MEMS pressure sensors for aerospace applications," *IEEE Aerospace Conference*, 1998, 1: 429–436.

[3] B. Folkmer, P. Steiner, and W. Lang, "A pressure sensor based on a nitride membrane using single-crystalline piezoresistors," *Sensors and Actuators A: Physical*, 1996, 54(1–3): 488–492.

[4] A. Berns, U. Buder, E. Obermeier, A. Wolter, and A. Leder, "Aero MEMS sensor array for high-resolution wall pressure measurements," *Sensors and Actuators A: Physical*, 2006, 132(1): 104–111.

[5] A. Wisitsoraat, V. Patthanasetakul, T. Lomas, and A. Tuantranont, "Low cost, thin film based piezoresistive MEMS tactile sensor," *Sensors and Actuators A: Physical*, 2007, 139(1–2): 17–22.

[6] R. E. Oosterbroek, T. S. J. Lammerink, J. W. Berenschot, G. J. M. Krijnen, M. C. Elwenspoek, and A. V. D. Berg, "A micromachined pressure/flow-sensor," *Sensors and Actuators A: Physical*, 1999, 77(3): 167–177.

[7] P. D. Dimitropoulos, C. Kachris, D. P. Karampatzakisa, and G. I. Stamoulis, "A new SOI monolithic capacitive sensor for absolute and differential pressure measurements," *Sensors and Actuators A: Physical*, 2005, 123–124: 36–43.

[8] L, Chen and M. Mehregany, "A silicon carbide capacitive pressure sensor for in-cylinder pressure measurement," *Sensors and Actuators A: Physical*, 2008, 145–146: 2–8.

[9] K. J. Suja, B. P. Chaudhary, and R. Komaragiri, "Design and simulation of pressure sensor for ocean depth measurement," *Applied Mechanics and Materials*, 2013, 313–314: 666–670.

[10] Y. Kanda and A. Yasukawa, “Optimum design considerations for silicon piezoresistive pressure sensors,” *Sensors and Actuators A: Physical*, 1997, 62(1–3): 539–542.

[11] K. Sakurano, H. Katoh, Y. Chun, and H. Watanabe, “Operation of a work function type SOI temperature sensor up to 250AC,” in *IEEE International SOI Conference Proceedings 2007*, Osaka, Japan, pp. 149–150, 2007.

[12] R. Sathishkumar, A. Vimalajuliet, J. S. Prasath, K. Selvakumar, and S. V. Reddy, “Micro size ultrasonic transducer for marine applications,” *Indian Journal of Science and Technology*, 2011, 4(1): 8–11.

[13] I. Obieta, E. Castano, and F. J. Gracia, “High temperature polysilicon pressure microsensor,” *Sensors and Actuators A: Physical*, 1995, 46(1–3): 161–165.

[14] S. Aravamudhan and S. Bhansali, “Reinforced piezoresistive pressure sensor for ocean depth measurements,” *Sensors and Actuators A: Physical*, 2008, 142(1): 111–117.

[15] M. Narayanaswamy, R. J. Daniel, K. Sumangala, and C. A. Jeyasehar, “Computer aided modelling and diaphragm design approach for high sensitivity silicon-on-insulator pressure sensor,” *Measurement*, 2011, 44(10): 1924–1936.

[16] L. Zhao, C. Xu, and G. Shen, “Analysis for load limitation of square-shaped silicon diaphragms,” *Solid-State Electronics*, 2006, 50(9–10): 1579–1583.

[17] S. Timoshenko and S. Woinowsky-Krieger, *Theory of Plates and Shells*. New York: McGraw-Hill, 1959: 16–20.

[18] Sreenath L.S, *Advanced Solid Mechanics*. New York: Tata MC Graw-Hill Education, 2001.